

Meson spectra of asymptotically free gauge theories from holographyJohanna Erdmenger,^{1,*} Nick Evans,^{2,†} and Marc Scott^{2,‡}¹*Max-Planck-Institut für Physik (Werner-Heisenberg-Institut),
Föhringer Ring 6, D-80805 Munich, Germany*²*STAG Research Centre and Physics & Astronomy, University of Southampton,
Southampton SO17 1BJ, United Kingdom*

(Received 9 January 2015; published 3 April 2015)

Using holography, we study the low-lying mesonic spectrum of a range of asymptotically free gauge theories. First, we revisit a simple top-down holographic model of QCD-like dynamics with predictions in the M_ρ - M_π plane. The meson masses in this model are in very good agreement with lattice gauge theory calculations in the quenched approximation. We show that the key ingredient for the meson mass predictions is the running of the anomalous dimension of the quark condensate γ . This provides an explanation for the agreement of holographic and quenched lattice gauge theory calculations. We then study the “dynamic AdS/QCD model,” in which the gauge theory dynamics is included by a choice for the running of γ . We use the naive two-loop perturbative running of the gauge coupling extrapolated to the nonperturbative regime to estimate the running of γ across a number of theories. We consider models with quarks in the fundamental, adjoint, two-index symmetric and two-index antisymmetric representations. We display predictions for M_ρ , M_π , M_σ and the lightest glueball mass. Many of these theories, where the contribution to the running of γ is dominated by the gluons, give very similar spectra, which also match with lattice expectations for QCD. On the other hand, a significant difference between spectra in different holographic models is seen for theories where the quark content changes the gradient of the running of γ around the scale at which chiral symmetry breaking is triggered at $\gamma \simeq 1$. For these walking theories, we see an enhancement of the ρ mass and a suppression of the σ mass. Both phenomena are characteristic for walking behavior in the physical meson masses.

DOI: [10.1103/PhysRevD.91.085004](https://doi.org/10.1103/PhysRevD.91.085004)

PACS numbers: 12.10.Dm, 11.25.Tq

I. INTRODUCTION

Asymptotically free gauge theories are notoriously difficult to study, since they run to strong coupling in the infrared. Computing the bound state spectrum of theories such as QCD is therefore very hard. First-principle lattice calculations are possible but very numerically expensive. They are typically guided by the answers observed in nature. It is hard to explore the range of behavior across the full space of asymptotically free theories. The holographic description of large N_c $\mathcal{N} = 4$ gauge theory [1] has raised the prospect of a dual gravitational picture for these theories in which the spectrum might be computed in a purely classical theory. Top-down attempts [2–4] to rigorously find a gravity dual originating from ten-dimensional string theory are complicated by the need to find a brane construction that decouples all unwanted superpartners, and also by the challenge of finding the appropriate gravitational background for embedding those branes. In any case, when the gauge theory is weakly coupled, such as in the ultraviolet, the gravitational theory will itself become strongly coupled.

Bottom-up holographic modeling [5] has taken broad-brushstroke lessons from the AdS/CFT correspondence and attempted to model the mesonic and glueball degrees of freedom. Basic AdS/QCD models appear to work reasonably well, even at the quantitative 10% level or better, but are not systematically improvable. This is due to the fact that in principle, very many operators and higher-dimensional couplings can be important for the vacuum and bound state structure. Both top-down and bottom-up models have therefore struggled to encode the particular dynamics of a specific theory with, for example, a definite value of N_c or the number of quark flavors N_f .

Recently there have been new attempts to construct holographic models [6–8] that address these issues and provide insight into why some top-down models give good descriptions of the QCD spectrum [9]. Here we will push these insights further with two goals: First, we provide further support for the success of an existing top-down model. Second, we present bottom-up models for a large range of different gauge theories. One key observation was highlighted already in Ref. [7], where it was noted in particular that the quark condensate that characterizes the vacuum in all such models is described holographically by a scalar in an AdS-like space. The scalar becomes unstable to acquiring a vacuum expectation value, corresponding to a quark condensate, when its mass violates the Breitenlohner-Freedman (BF)

*jke@mpp.mpg.de
†evans@soton.ac.uk
‡m.scott@soton.ac.uk

bound [10]. This mass bound is given by $m^2 = -4$ in AdS₅, for instance. The AdS mass of the scalar in turn is mapped by the AdS/CFT dictionary [1] to the dimension of the gauge theory operator, $m^2 = \Delta(\Delta - 4)$. This implies that in a dual to a QCD-like theory, the operator $\bar{q}q$ operator has dimension three in the UV and is described by a scalar with $m^2 = -3$. To reach the BF bound, beyond which there is an instability leading to condensation to a new ground state and chiral symmetry breaking, the dimension of $\bar{q}q$ must have become $\Delta = 2$, which corresponds to an anomalous dimension of $\gamma = 1$. Top-down holographic models of QCD-like theories that use probe branes display the importance of these ideas: as described in Ref. [9], the running of the coupling or factors deviating from AdS in the background metric enter into the Dirac-Born-Infeld (DBI) action of the probe that describes the quark and meson physics. If the DBI action is linearized, it leads to an action for a scalar in AdS, dual to the operator describing $\bar{q}q$, with a running mass squared. This effective running mass is generated by the metric and forms of the background geometry which enter the DBI action. In fact, the dual geometry and running of the coupling enter into the effective AdS/QCD model only through the running of the anomalous dimension γ , i.e. of the mass squared of the AdS scalar.

Models that describe QCD reasonably have $\gamma = 0$ in the UV (as occurs naturally in a theory that is supersymmetric in the UV), a long range over which γ is small, and a sudden rise to γ greater than 1. This running is broadly similar to that in QCD, where the logarithmic running keeps γ small except around Λ_{QCD} , where it blows up rapidly. We will illustrate this here in the top-down Constable-Myers model [4, 11], which has been highlighted in Ref. [3] as providing a surprisingly good description relative to lattice data of the light spectrum.

These ideas were simplified in Ref. [8], where the “dynamic AdS/QCD” model was proposed. The model is just the linearized DBI action of the D3/probe-D7 system, but with an arbitrary running for γ . To describe any particular gauge theory, then, requires a guess as to the form of that running. A naive but still sensible guess is provided by the perturbative running of the QCD coupling to two loops. For N_f just below $11N_c/2$, where asymptotic freedom is gained, the two-loop running displays a Banks-Zaks fixed point [12]. As N_f is decreased, the value of the coupling at the fixed point increases and the anomalous dimension γ increases. At a point close to $N_f \simeq 4N_c$ for fundamental quarks, the BF bound is tripped and chiral symmetry breaking sets in. Above that value of N_f , the model is in the regime referred to as the “conformal window” [13]. Using the standard AdS relations, the running can be translated into a radially dependent mass squared for the scalar describing the condensate. The model then makes predictions for the spectrum of the theory. Here we will concentrate on the ρ meson, the pions, the σ meson (i.e. the singlet $\bar{q}q$ bound state with vanishing quantum numbers, also identified with the f_0), and the lightest glueball.

For the glueball, only qualitative statements are possible, since the dynamic AdS/QCD model concentrates on the quark sector. We will present our results in the style of “Edinburgh” plots [14] used by lattice gauge theorists. These plots display only physical observables, such as the mass of the ρ as function of the pion mass, in order to remove scheme-dependent quantities such as the quark mass.

In our Sec. II, we will revisit the Constable-Myers model of chiral symmetry breaking [4, 11] and extract, by linearizing the DBI action of a D7 brane in the geometry, the running anomalous dimension. We will show that in the critical range of radial coordinate, where $\gamma \simeq 1$, the running of the model is similar to quenched QCD. We compare the M_ρ against M_π behavior with that of quenched lattice computations [15] and reemphasize the surprising success of the model. In the subsequent sections, we then turn to the dynamic AdS/QCD model [8], which allows us to explore the space of gauge theories as a function of N_c , N_f and the dependence on the representation of the quarks. Again we find the holographic models give good agreement with lattice data where it exists. In fact, we find a relatively weak dependence on N_c and the quark representation. Significant deviations from QCD-like behavior are seen for so-called “walking” gauge theories [16]. These are theories whose running is governed by an IR fixed point, although this point is never reached due to chiral symmetry breaking. Moreover, these theories approach fixed points with γ close to but above 1 since they exist for N_f just below $N_f \simeq 4N_c$. For these theories, the gradient of γ as function of the running coupling is small when $\gamma = 1$. They are expected to have a quark condensate which is enhanced in the UV, which in turn tends to enhance the ρ mass, enhance the π mass to a lesser degree, and suppress the σ mass [17, 18]. The effective potential becomes very flat as the UV condensate is pushed out to high scales, leaving a pseudo-flat radial direction in the potential. We observe all of these phenomena in our model.

These models remain only models though, since they cannot be brought closer to the true dynamics systematically, and they depend on the naive guess for the running of γ . Indeed, in gauge theory beyond two loops, the running parameters are gauge dependent, but we hope working at lower order does correctly capture the dynamics of the gauge theory running. Nevertheless, the success in reproducing the lattice data, where such data exist, gives hope that the approach presented provides information about universal behavior in these theories. In particular, we hope that the trends we see as the edge of the conformal window is reached will provide guidance to lattice simulations of those theories [19].

II. A TOP-DOWN MODEL

An early holographic description of QCD [4] was provided by placing D7-brane probes in the dilaton flow geometry of Constable and Myers [11]. D3-D7 strings

introduce quenched quark degrees of freedom. The Constable-Myers deformation of $\text{AdS}_5 \times \text{S}^5$ is a very simple description of a gauge theory with a running coupling that breaks the $\mathcal{N} = 4$ supersymmetry completely. The nontrivial dilaton profile is dual to that running coupling and has an IR pole which is ill understood. In practice, the geometry describes a gravity dual of a soft wall, since the singularity is repulsive to probe branes. The D7 probes bend away from the singularity, and asymptotically the embedding describes a dynamically generated quark condensate at zero quark mass. In Ref. [3], the light meson spectrum was computed. Moreover, the M_ρ versus M_π^2 plot was compared to quenched lattice data [15]. We update these computations in Fig. 1. The fit is remarkably good. At the time, this seemed very surprising, since the gauge theory apparently lies close to infinitely strongly coupled $\mathcal{N} = 4$ gauge theory with all the associated superpartners and has no asymptotic freedom. In this section, we return to this model and analyze it in the spirit of Ref. [9] to shed some light on the success at describing the QCD spectrum.

The gravity background of Constable and Myers [11] in an Einstein frame has the geometry

$$ds^2 = H^{-1/2} \left(\frac{w^4 + b^4}{w^4 - b^4} \right)^{\delta/4} \sum_{j=0}^3 dx_j^2 + H^{1/2} \left(\frac{w^4 + b^4}{w^4 - b^4} \right)^{(2-\delta)/4} \frac{w^4 - b^4}{w^4} \sum_{i=1}^6 dw_i^2, \quad (1)$$

where b is the scale of the geometry that determines the size of the deformation [$\delta = R^4/(2b^4)$ with R the AdS radius], and

$$H = \left(\frac{w^4 + b^4}{w^4 - b^4} \right)^\delta - 1, \quad w^2 = \sum_{i=1}^6 w_i^2. \quad (2)$$

In this coordinate system, the dilaton and four-form are, with $\Delta^2 + \delta^2 = 10$,

$$e^{2\Phi} = e^{2\Phi_0} \left(\frac{w^4 + b^4}{w^4 - b^4} \right)^\Delta, \quad (3)$$

$$C_{(4)} = -\frac{1}{4} H^{-1} dt \wedge dx \wedge dy \wedge dz.$$

This geometry returns to $\text{AdS}_5 \times \text{S}^5$ in the UV, as may be seen by explicitly expanding at large radial coordinate w .

To add quarks [4], we will use an embedded probe D7-brane. The D7-brane will be embedded with world-volume coordinates identified with $x_{0,1,2,3}$ and $w_{1,2,3,4}$. Transverse fluctuations will be parametrized by w_5 and w_6 (or L and ϕ in polar coordinates)—it is convenient to define a coordinate ρ such that $\sum_{i=1}^4 dw_i^2 = d\rho^2 + \rho^2 d\Omega_3^2$ and

the radial coordinate is given by $w^2 = \rho^2 + w_5^2 + w_6^2 = \rho^2 + L^2$.

The Dirac-Born-Infeld action of the D7-brane probe in the Constable-Myers background takes the form

$$S_{D7} = -T_7 R^4 \int d^8 \xi \epsilon_3 e^\phi \mathcal{G}(\rho, L) (1 + g^{ab} g_{LL} \partial_a L \partial_b L + g^{ab} g_{\phi\phi} \partial_a \phi \partial_b \phi + 2\pi\alpha' F^{ab})^{1/2}, \quad (4)$$

where

$$\mathcal{G} = \rho^3 \frac{((\rho^2 + L^2)^2 + b^4)((\rho^2 + L^2)^2 - b^4)}{(\rho^2 + L^2)^4}.$$

Here we have rescaled w and b in units of R , so that factors of R only occur as an overall factor on the embedding Lagrangian.

From these equations we derive the corresponding equation of motion. We look for classical solutions of the form $L(\rho)$, $\phi = 0$. Numerically, we shoot from a regular boundary condition in the IR ($L' = 0$) and find solutions with the asymptotic behavior $L \sim m + c/\rho^2$. These coefficients are then identified with the quark mass and condensate $\langle \bar{\psi}\psi \rangle$, respectively (formally c is only the unique contribution to the condensate in the zero-mass limit [20]), in agreement with the usual AdS/CFT dictionary obtained from the asymptotic boundary behavior.

Mesonic states are identified by looking at linearized fluctuations about the background embedding. Fluctuations in ϕ correspond to the pion, and fluctuations in the world volume gauge field correspond to the ρ meson. In each case one seeks solutions of the form $f(\rho)e^{ik \cdot x}$, $k^2 = -M^2$, with the mass states being picked out by the condition that $f(\rho)$ is regular.

Figure 1 shows the first example of the plots we will be producing in this paper—it shows the ρ -meson mass as a function of the pion mass squared. Note that in any given theory we must fix the strong coupling scale Λ . Here and throughout this paper, we choose to do this by setting the ρ mass at $M_\pi = 0$ (i.e. when the quark mass is zero) to be the same in all theories, and we express all physical quantities in units of that fixed mass. The figure shows the results from the Constable-Myers model. We also display quenched lattice results for the plot in theories with gauge group $\text{SU}(3)$, $\text{SU}(5)$ and $\text{SU}(7)$ —data taken from Ref. [15]. Note that in order to place the lattice data on the plot, we have taken the two data points at lowest M_π and linearly extrapolated to find M_ρ at $M_\pi = 0$. This is naive, and we will argue later that this may put the points a little high in the plane. Conservatively, we will use the spread of the lattice data across the different $\text{SU}(N_c)$ theories as reflective of the systematic errors in the lattice simulations. The remarkable thing is the lack of dependence on N_c in the lattice data and the match of the holographic model to the lattice data. The aim of this section is to identify why there

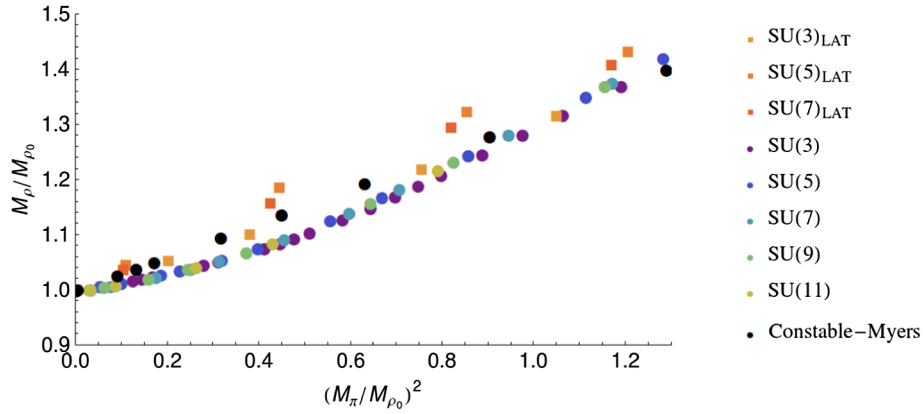


FIG. 1 (color online). Plots of M_ρ against M_π^2 : In each case, the points are normalized by M_ρ at $M_\pi = 0$ to set the nonperturbative scale Λ . As shown in the key, the plot shows the data for quenched lattice computations taken from Ref. [15] (and linearly fitted to find M_ρ at $M_\pi = 0$), the Constable-Myers top-down model, and the dynamic AdS/QCD predictions.

is such a close match given the large deviations in the holographic dual that includes different adjoint particle content and UV behavior.

Following Ref. [9], we will argue that the key element for the quark physics in the top-down model is the running of the anomalous dimension γ with the renormalization scale. We will show that this running is very similar to that in QCD, especially in the regime where $\gamma \approx 1$ and where the BF bound-violating instability sets in that causes chiral symmetry breaking. To study this instability we will look at when the chirally symmetric $L = 0$ embedding becomes unstable. We simply take our DBI action, which up to a multiplicative constant we may write as

$$S_{D7} = \int d\rho \lambda(\rho, L) \rho^3 \sqrt{1 + (\partial_\rho L)^2}, \quad (5)$$

where $\lambda(\rho, L) = \rho^{-3} e^{\phi} \mathcal{G}(\rho, L)$ and $r = \sqrt{\rho^2 + L^2}$, and expand around $L = L' = 0$ to quadratic order:

$$\begin{aligned} S_{D7} &= \int d\rho \rho^3 \left(\lambda|_{L=0} + \frac{\partial \lambda}{\partial L^2} \Big|_{L=0} L^2 \right) \left(1 + \frac{1}{2} (\partial_\rho L)^2 \right), \\ &= \int d\rho \rho^3 \left(\frac{1}{2} \lambda|_{L=0} (\partial_\rho L)^2 + \partial_{L^2} \lambda|_{L=0} L^2 \right). \end{aligned} \quad (6)$$

In order to ensure that the kinetic term in our Lagrangian is canonical, we perform a coordinate transformation on ρ ,

$$\lambda(\rho) \rho^3 \frac{\partial}{\partial \rho} \equiv \tilde{\rho}^3 \frac{\partial}{\partial \tilde{\rho}}; \quad (7)$$

that is,

$$\tilde{\rho} = \sqrt{\frac{1}{2} \int_\rho^\infty \frac{1}{\lambda \rho^3} d\rho}. \quad (8)$$

We may rewrite our action in terms of the $\tilde{\rho}$ variable. Along with writing $L(\rho) = \tilde{\rho} \phi(\tilde{\rho})$, we obtain

$$S_{D7} = \int d\tilde{\rho} \frac{1}{2} \tilde{\rho}^3 \left(\tilde{\rho}^2 (\partial_{\tilde{\rho}} \phi)^2 + 3\phi^2 + \lambda \frac{\partial \lambda}{\partial \rho} \Big|_{L=0} \frac{\rho^5}{\tilde{\rho}^4} \phi^2 \right). \quad (9)$$

The first two terms in the action describe a canonical $m^2 = -3$ scalar in AdS₅, whereas the remaining term gives a ρ -dependent mass to the scalar field in AdS₅. We find an overall mass squared

$$m^2 = -3 - \delta m^2, \quad \delta m^2 \equiv -\lambda \frac{\partial \lambda}{\partial \rho} \Big|_{L=0} \frac{\rho^5}{\tilde{\rho}^4}. \quad (10)$$

Using the standard scalar mass/operator dimension relation of the AdS/CFT dictionary, $m^2 = \Delta(\Delta - 4)$, but now assuming the mass dimension of the $q\bar{q}$ operator to be $3 - \gamma$, where γ is the running anomalous dimension of the gauge theory quark mass, we obtain the relation

$$m^2 = -3 - 2\gamma + \gamma^2. \quad (11)$$

Thus we associate $\delta m^2 = -2\gamma + \gamma^2$, and are thus able to extract a running anomalous dimension in the Constable-Myers background.

The key point to note is that the only way that the background geometry and running dilaton enters into the equation for the embedding is through the running of γ . The background D7 embedding is then the key ingredient for the computation of linearized fluctuations that determine the mesonic masses. Effectively, the origin of the running of γ is lost—so questions about whether the background has too many superpartners of the gauge fields, or whether the running coupling is correctly that of QCD in the UV, and so forth, become subsumed into simply asking whether γ is close to that in QCD.

In Fig. 2, we plot the RG scale dependence of the anomalous dimension γ extracted from the Constable-Myers model and the one-loop running of large- N_c quenched QCD theory. We have matched the strong coupling scale of the two theories by assuming that they each take the value $\gamma = 1$ at the same scale. Setting the AdS

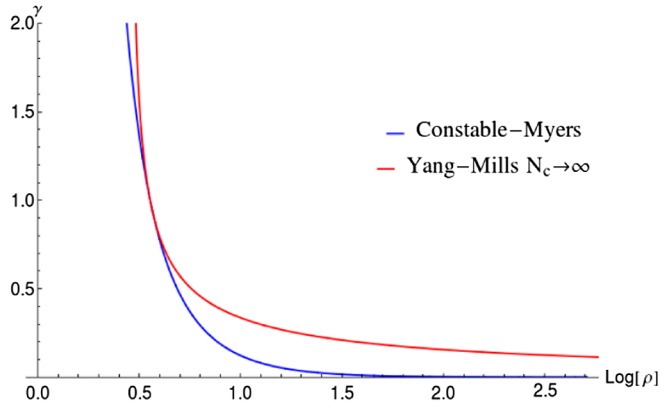


FIG. 2 (color online). A plot of the anomalous dimension γ in the top-down Constable-Myers model. It is compared to QCD by using the one-loop perturbative result for the running coupling in large- N_c Yang-Mills theory ($\mu d\alpha/d\mu = -11N_c\alpha^2/6\pi$) as input for calculating the anomalous dimension γ [$\gamma = 3N_c\alpha(\mu)/4\pi$]. We set the scale at which $\gamma = 1$ to be equal in each case.

radius R to 1, we identify the RG scale and the radial coordinate by $\mu = \ln \rho$ (i.e., we are choosing to set this relation by matching to the physical RG scale). This is the scale where chiral symmetry breaking is triggered, in the holographic model by the BF bound violation. From the figure it is immediately obvious that the scale dependence of the anomalous dimension γ is similar in both cases, and the gradient of γ is almost the same near $\gamma = 1$. Deviations in the UV are present but are mild. They occur in the regime where the BF bound is not violated in the holographic model.

This close matching of the scale dependence of the anomalous dimension is, we believe, the reason for the success of the holographic model. It is worth pointing out that the reason that the holographic description and QCD match in the UV is somewhat artificial. The UV of the Constable-Myers theory is infinitely strongly coupled $\mathcal{N} = 4$ super Yang-Mills theory, yet the theory's large amount of supersymmetry preserves the perturbative dimension of the quark operator, i.e. $\gamma = 0$. In QCD, the UV result $\gamma = 0$ simply follows from weak coupling. This coincidence has long been behind the successes of AdS/QCD models.

Given that the key ingredient to describe the mesonic spectrum is simply the running of γ , it seems an obvious step to do away with the background construction of a geometry that mimics QCD, since there is no top-down holographic construction of real QCD, and to simply use the assumed form of γ as an input in the DBI action. This is essentially the starting point for the bottom-up model that we call “dynamic AdS/QCD” [8], which we will now move to studying.

III. DYNAMIC AdS/QCD

Dynamic AdS/QCD was introduced in detail in Ref. [8]. The model maps onto the action of a probe D7 brane in an

AdS geometry expanded to quadratic order [9]. The anomalous dimension of the quark mass/condensate is encoded through a mass term that depends on the radial AdS coordinate ρ .

The five-dimensional action of our effective holographic theory is

$$S = \int d^4x d\rho \text{Tr} \rho^3 \left[\frac{1}{\rho^2 + |X|^2} |DX|^2 + \frac{\Delta m^2}{\rho^2} |X|^2 + \frac{1}{2} F_V^2 \right]. \quad (12)$$

The field X (the equivalent of the embedding coordinates L, ϕ of the D7 brane in the top-down model) describes the quark condensate degree of freedom. Fluctuations in $|X|$ around its vacuum configurations describe the scalar meson. The π fields are the phase of X ,

$$X = L(\rho) e^{2i\pi^a T^a}. \quad (13)$$

F_V are vector fields that will describe the vector (V) mesons.

We work with the five-dimensional metric

$$ds^2 = \frac{d\rho^2}{(\rho^2 + |X|^2)} + (\rho^2 + |X|^2) dx^2, \quad (14)$$

which will be used for contractions of the space-time indices. ρ is the holographic coordinate, and $|X| = L$ enters into the effective radial coordinate in the space, i.e. there is an effective $r^2 = \rho^2 + |X|^2$. This is how the quark condensate generates a soft IR wall for the linearized fluctuations that describe the mesonic states: when L is nonzero the theory will exclude the deep IR at $r = 0$.

The normalizations of X and F_V are determined by matching to the gauge theory in the UV. External currents are associated with the non-normalizable modes of the fields in AdS. In the UV we expect $|X| \sim 0$, and we can solve the equations of motion for the scalar $L = K_S(\rho) e^{iq \cdot x}$ and vector $V^\mu = \epsilon^\mu K_V(\rho) e^{iq \cdot x}$ fields. Each satisfies the same equation,

$$\partial_\rho [\rho^2 \partial_\rho K] - \frac{q^2}{\rho} K = 0. \quad (15)$$

The UV solution is

$$K_i = N_i \left(1 + \frac{q^2}{4\rho^2} \ln(q^2/\rho^2) \right), \quad (i = S, V), \quad (16)$$

where N_i are normalization constants that are not fixed by the linearized equation of motion. Substituting these solutions back into the action gives the scalar correlator Π_{SS} and the vector correlator Π_{VV} . Performing the usual matching to the UV gauge theory requires us to set

$$N_S^2 = N_V^2 = \frac{N_c N_f}{24\pi^2}. \quad (17)$$

The vacuum structure of the theory can be determined by setting all fields except $|X| = L$ to zero. We assume that L will have no dependence on the x coordinates. The action for L is given by

$$S = \int d^4x d\rho \rho^3 \left[(\partial_\rho L)^2 + \Delta m^2 \frac{L^2}{\rho^2} \right]. \quad (18)$$

If $\Delta m^2 = 0$, then the scalar, L , describes a dimension-3 operator and dimension-1 source as is required for it to represent $\bar{q}q$ and the quark mass m . That is, in the UV the solution for the L equation of motion is $L = m + \bar{q}q/\rho^2$. A nonzero Δm^2 allows us to introduce an anomalous dimension for this operator. If the mass squared of the scalar violates the BF bound of -4 ($\Delta m^2 = -1$, $\gamma = 1$), then the scalar field L becomes unstable and the theory enters a chiral-symmetry-breaking phase.

We will fix the form of Δm^2 using the two-loop running of the gauge coupling in QCD with N_f flavors transforming under a representation R . This takes the form

$$\mu \frac{d\alpha}{d\mu} = -b_0 \alpha^2 - b_1 \alpha^3, \quad (19)$$

where

$$b_0 = \frac{1}{6\pi} \left(11C_2(G) - 4N_f C_2(R) \frac{\dim(R)}{\dim(G)} \right), \quad (20)$$

and

$$b_1 = \frac{1}{8\pi^2} \left(\frac{34}{3} [C_2(G)]^2 - \left[\frac{20}{3} C_2(G)C_2(R) + 4[C_2(R)]^2 \right] \times N_f \frac{\dim(R)}{\dim(G)} \right). \quad (21)$$

Above, we denote the adjoint representation as G and its respective Casimir by $C_2(G) = N_c$. Table I shows all the distinguishing quantities associated with each of the representations we consider: the dimension of the representation, $C_2(R)$, and the minimum number of flavors required for loss of asymptotic freedom, N_f^{\max} .

The one-loop result for the anomalous dimension of the quark mass is

$$\gamma_1(\mu; R) = \frac{3C_2(R)}{2\pi} \alpha(\mu; R). \quad (22)$$

We will identify the RG scale μ with the AdS radial parameter $r = \sqrt{\rho^2 + L^2}$ in our model. Note that it is important that L enter here. If it did not and the scalar mass were only a function of ρ , then were the mass to violate the

TABLE I. Distinguishing quantities of representations of $SU(N_c)$ gauge theories with asymptotic freedom valid for any $N_c \geq 2$.

| R | $\dim(R)$ | $C_2(R)$ | N_f^{\max} |
|-------------|------------------------|------------------------------|----------------------------------|
| Fundamental | N_c | $\frac{N_c^2-1}{2N_c}$ | $\frac{11}{2} N_c$ |
| Adjoint (G) | $N_c^2 - 1$ | N_c | $2\frac{3}{4}$ |
| 2IS | $\frac{N_c(N_c+1)}{2}$ | $\frac{(N_c-1)(N_c+2)}{N_c}$ | $\frac{11}{2} \frac{N_c}{N_c+2}$ |
| 2IA | $\frac{N_c(N_c-1)}{2}$ | $\frac{(N_c+1)(N_c-2)}{N_c}$ | $\frac{11}{2} \frac{N_c}{N_c-2}$ |

BF bound at some ρ , it would leave the theory unstable however large L grew. Including L means that the creation of a nonzero but finite L can remove the BF bound violation, leading to a stable solution. This is analogous to what happens in the top-down model.

Working perturbatively from the AdS result $m^2 = \Delta(\Delta - 4)$, we have

$$\Delta m^2 = -2\gamma_1(\mu; R) = -\frac{3C_2(R)}{\pi} \alpha(\mu; R). \quad (23)$$

This will then fix the r dependence of the scalar mass through Δm^2 as a function of N_c and N_f for each R . Note that if one were to attempt such a matching beyond two-loop order, the perturbative result would become gauge dependent. We hope that the lower-order gauge-independent results provide sensible insight into the running in the theory.

It is important to stress that using the perturbative result outside the perturbative regime is in no sense rigorous, but simply a phenomenological parametrization of the running as a function of μ, N_c, N_f that shows fixed-point behavior. We expect broad trends in the behavior of the theories with varying N_f, N_c to be sensibly described with this ansatz. Similarly, the relation (23) between Δm^2 and γ_1 is a guess outside of the perturbative regime. Note that the holographic fixed point value for the anomalous dimension is given by solving $\Delta(\Delta - 4) = \Delta m^2$, and the resultant γ will not be the same as the fixed point in γ_1 away from the perturbative regime.

The vacuum structure for a given choice of representation, N_f and N_c , must be identified first. The Euler-Lagrange equation for the vacuum embedding L_v is given at fixed Δm^2 by the solution of

$$\frac{\partial}{\partial \rho} (\rho^3 \partial_\rho L_v) - \rho \Delta m^2 L_v = 0. \quad (24)$$

Note that if Δm^2 depends on L at the level of the Lagrangian, then there would be an additional term $-\rho L_v^2 \partial \Delta m^2 / \partial L_v$. We neglect this term and instead impose the running of Δm^2 at the level of the equation of motion. The reason is that the extra term introduces an effective

contribution to the running of γ that depends on the gradient of the running coupling. Such a term is not present in perturbation theory in our QCD-like theories—we wish to keep the running of γ in the holographic theory as close to the perturbative guidance from the gauge theory as possible.

In order to find $L_v(\rho)$, we solve the equation of motion numerically with shooting techniques with an input IR initial condition. A sensible first guess for the IR boundary condition is

$$L_v(\rho = L_0) = L_0, \quad L'_v(\rho = L_0) = 0. \quad (25)$$

This IR condition is similar to that from top-down models [2] but imposed at the RG scale, where the flow becomes “on mass shell.” Here we are treating $L_v(\rho)$ as a constituent quark mass at each scale ρ . Were we to continue the flow below this quark mass scale, we would need to address the complicated issue of the decoupling of the quarks from the running function γ .

A. Meson spectra

We now turn to computing the physical parameters, the masses of the (ρ, σ, π) -mesons and the scalar glueball, for each viable representation. These parameters are true predictions of the model which, just as in the gauge theories, depend only on the choice of the quark mass, N_c , N_f and the scale Λ .

B. Linearized fluctuations

The isoscalar $\bar{q}q$ (σ) mesons are described by linearized fluctuations of L about its vacuum configuration, L_v . We look for space-time-dependent excitations, i.e. $|X| = L_v + \delta(\rho)e^{iq \cdot x}$, $q^2 = -M_\sigma^2$. The equation of motion for δ is, linearizing (24),

$$\begin{aligned} \partial_\rho(\rho^3 \delta') - \Delta m^2 \rho \delta - \rho L_v \delta \frac{\partial \Delta m^2}{\partial L} \Big|_{L_v} \\ + M_\sigma^2 R^4 \frac{\rho^3}{(L_v^2 + \rho^2)^2} \delta = 0. \end{aligned} \quad (26)$$

We seek solutions with, in the UV, asymptotics of $\delta = \rho^{-2}$ and with $\partial_\rho \delta|_{L_0} = 0$ in the IR, giving a discrete meson spectrum.

The isovector (ρ) meson spectrum is determined from the normalizable solution of the equation of motion for the spatial pieces of the vector gauge field $V_{\mu\perp} = \epsilon^\mu V(\rho)e^{iq \cdot x}$ with $q^2 = -M^2$. The appropriate equation is

$$\partial_\rho[\rho^3 \partial_\rho V] + \frac{\rho^3 M^2}{(L_v^2 + \rho^2)^2} V = 0. \quad (27)$$

We again impose $\partial_\rho V|_{L_0} = 0$ in the IR and require in the UV that $V \sim c/\rho^2$.

The pion mass spectrum is identified by assuming a space-time-dependent phase $\pi^a(x)$ of the AdS scalar X describing the $\bar{q}q$ degree of freedom, i.e. $X = L(\rho) \exp(2i\pi^a(x)T^a)$. The equation of motion of the pion field is then

$$\partial_\rho(\rho^3 L_v^2 \partial_\rho \pi^a) + M_\pi^2 \frac{\rho^3 L_v^2}{(\rho^2 + L_v^2)^2} \pi^a = 0. \quad (28)$$

Again, we impose at the IR boundary that $\partial_\rho \pi^a|_{L_0} = 0$.

C. Results

We can now move to displaying the outcomes of the dynamic AdS/QCD theory. We will fix the strong coupling scale Λ by fixing the ρ mass at $M_\pi = 0$ for each choice of representation, N_f and N_c , and express all quantities in units of that scale. For our plots, then, the only input parameters are the quark mass, N_f and N_c . We will explore a range of gauge theories with different quark matter.

1. Quenched fundamental representation

To test the model, we first compute M_ρ and M_π in the model with quenched fundamental quarks. This means that we do not include the quark contribution in the running of the gauge coupling. We compute the meson masses as functions of N_c to compare with the previously discussed quenched lattice data of Fig. 1. We display the data also in Fig. 1. We note that all choices of $SU(N_c)$ give essentially the same curve in this plot. This curve lies below, but within 5% of the prediction of the Constable-Myers top-down model. The result for the dynamic AdS/QCD model in this plot displays some curvature over the range of the lattice data, suggesting that the linear extrapolation used to place the lattice data on the plot may be incorrect. This suggests that the results for the lattice data in our linear fit are slightly too large, by as much as 5%. Indeed, in Ref. [15], evidence is presented for a nonlinear fit already in the lattice data. Given the expectation of some systematic error on the lattice data (see Ref. [15]), the match between all these models is remarkable and lends considerable support to further predictions of the dynamic AdS/QCD model.

To emphasize how well the results match, we also plot the same dynamic AdS/QCD and lattice data on a Log-Log plot in Fig. 3. The figure also displays the line $M_\rho = M_\pi$, which would be the one appropriate to a very weakly coupled theory where both mesons' masses are just twice the quark mass. This line is expected to be approached at large M_π , i.e. in the limit of large quark mass. Clearly, the very different computations for these theories agree rather well. While both the holographic models' curves are compatible with the lattice data at the level of the errors due to the coarse lattice spacing taken in Ref. [15], the

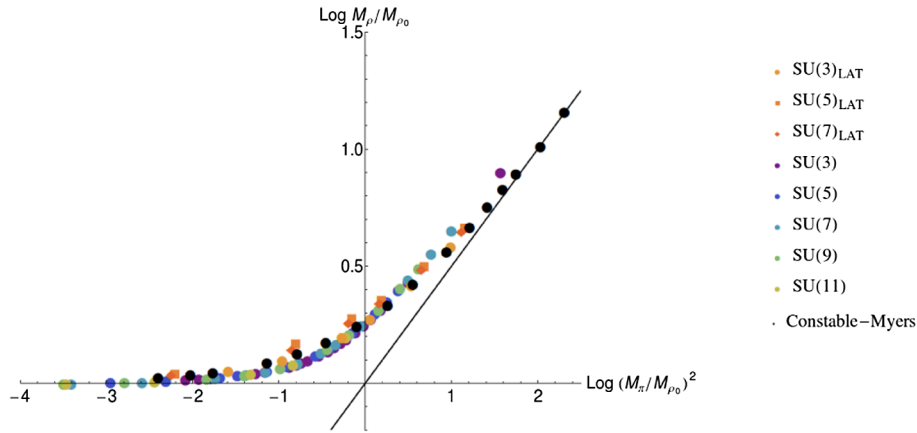


FIG. 3 (color online). A Log-Log plot of M_ρ versus M_π^2 : The plot displays the quenched lattice data from Ref. [15], the top-down Constable-Myers model of Sec. II and the quenched results for varying N_c in dynamic AdS/QCD from Sec. III. The solid line corresponds to $M_\rho = M_\pi$.

top-down Constable-Myers model does fit the data mildly better (the M_ρ points are raised by up to 2% or so), including in the large- M_π limit. If this is indeed the case, then it is likely due to γ in that model falling to zero more quickly than in QCD as a function of the RG scale—the holographic description of the UV is probably closer to perturbative QCD with $\gamma = 0$.

2. Fundamental representation

The quenched results display very little dependence on N_c . The reason is that the running of γ at the point $\gamma = 1$ is very fast in all these cases, so the dynamics comes out very similar. To see some N_c dependence, we should unquench the theory and include a sufficient number of quarks to affect the running. For example, in Fig. 4 we show the N_c variation in the M_ρ - M_π^2 plane of a theory with $N_f = 8$. The dependence on N_c is again not huge, but for low N_c there is a clear distinction from larger N_c theories that are effectively more quenched. This further emphasizes the success of the holographic model in lying so close to the quenched lattice data—it is not that the curves seen in the previous subsection are the only outcome.

We can now turn to studying the question of whether there are choices of N_f and N_c that provide spectra very different from QCD-like theories. As is well known, the theories that are most unlike QCD are those on the edge of the conformal window. For example, for an SU(3) gauge theory at $N_f > 12$, the running of γ flows to an IR fixed point below $\gamma = 1$. In the holographic model, the BF bound is not violated and chiral symmetry breaking does not occur. For theories that do break chiral symmetry at slightly lower values of N_f , the theory runs close to an IR fixed point that just violates the BF bound. Crucially, at the point where $\gamma = 1$, the gradient of the running of γ is much smaller than in QCD-like theories. To demonstrate the impact of this on the spectrum, we plot the N_f dependence

of the SU(3) theory in the M_ρ - M_π^2 plane in Fig. 5. The ρ mass is substantially enhanced relative to the π mass at larger N_f .

Theories with slow running at the scale where chiral symmetry breaking is triggered are called walking gauge theories [16]. For these theories, the chiral condensate has dimension approximately 2 at the IR scale of conformal symmetry breaking. The dimension-3 UV condensate is roughly the product of that dimension-2 IR condensate and the scale of the one-loop β function of the theory that determines where the anomalous dimension changes from

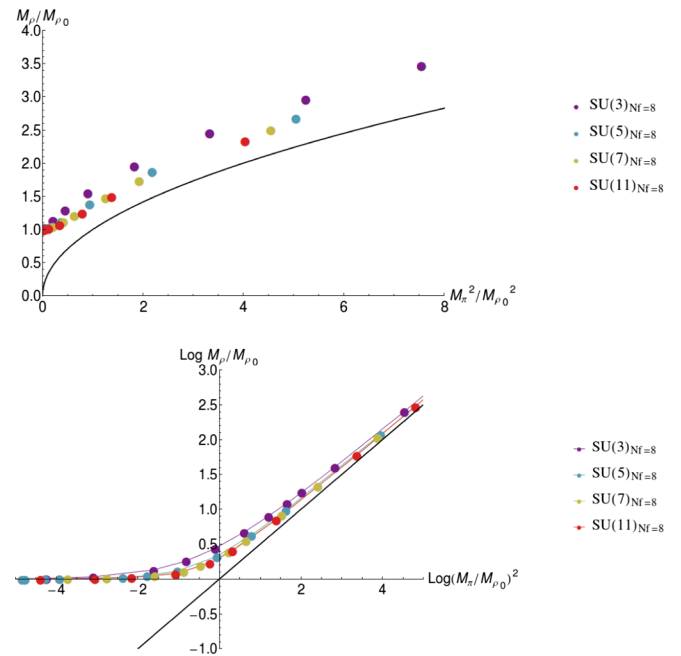


FIG. 4 (color online). M_ρ versus M_π^2 in SU(N_c) theory with $N_f = 8$ fundamental quarks: The lower plot shows the same in Log-Log format. The solid line corresponds to $M_\rho = M_\pi$.

$\gamma = 0$ to $\gamma = 1$. This scale will be much larger than the IR scale and the UV condensate enhanced. The usual expectation is that the ρ mass will be proportional to $\langle \bar{q}q \rangle^{1/3}$, while the π mass will scale as $m_q^{1/2} \langle \bar{q}q \rangle^{1/6}$. An enhancement of the condensate would therefore raise M_ρ at any fixed M_π , as is seen in Fig. 5. Generically, for different N_c we observe the same behavior as $N_f/N_c \rightarrow 4$.

This is a good point at which to compare our dynamic AdS/QCD theory to unquenched lattice data [21–23]. We have seen that the effect of including more quarks in our model is that the value of M_ρ rises at fixed M_π . This suggests that the effect of quark loops is to raise M_ρ . We display lattice data in the top plot of Fig. 5—we show both the quenched results previously discussed for SU(3) gauge theory, but now also unquenched data for the same theory with $N_f = 3$, taken from Refs. [21–23]. The three sets of lattice data show some spread in the low- M_π region, but we indeed observe a shift upwards in M_ρ by 20% or so. In fact, the fit to the dynamic AdS/QCD model for $N_f = 3$ is a little poorer than to the quenched lattice data—the lattice points are more similar to the $N_f = 5$ version of dynamic

AdS/QCD (although there is clearly some uncertainty in the lattice results as shown by the spread). This is most plausibly explained as a failure of the very naive perturbative-based running ansatz we have used as an input into the model. The key measure is the gradient of γ with RG scale at the scale where $\gamma = 1$. For $N_f = 3$, $\gamma' = -4.25$; while at $N_f = 5$, $\gamma' = -3.70$. This implies that the shift in spectrum is caused by a 15% shift in this gradient. Clearly the perturbative ansatz cannot be trusted at this level of accuracy. It is not surprising that the precise features of the spectrum are dependent on the choice of assumed running for γ . It is encouraging that the holographic model gets gross features correct, such as the rise in M_ρ in theories with more quark loops. This gives us confidence that the holographic model can be useful in understanding broad trends in the spectrum as the quark content of the theory is changed.

An additional expectation in a walking theory is that the σ -mode $\bar{q}q$ bound state should become light as one approaches the edge of the conformal window from below. The reason is that since the quark condensate is enhanced, the effective potential for the condensate becomes flatter, as

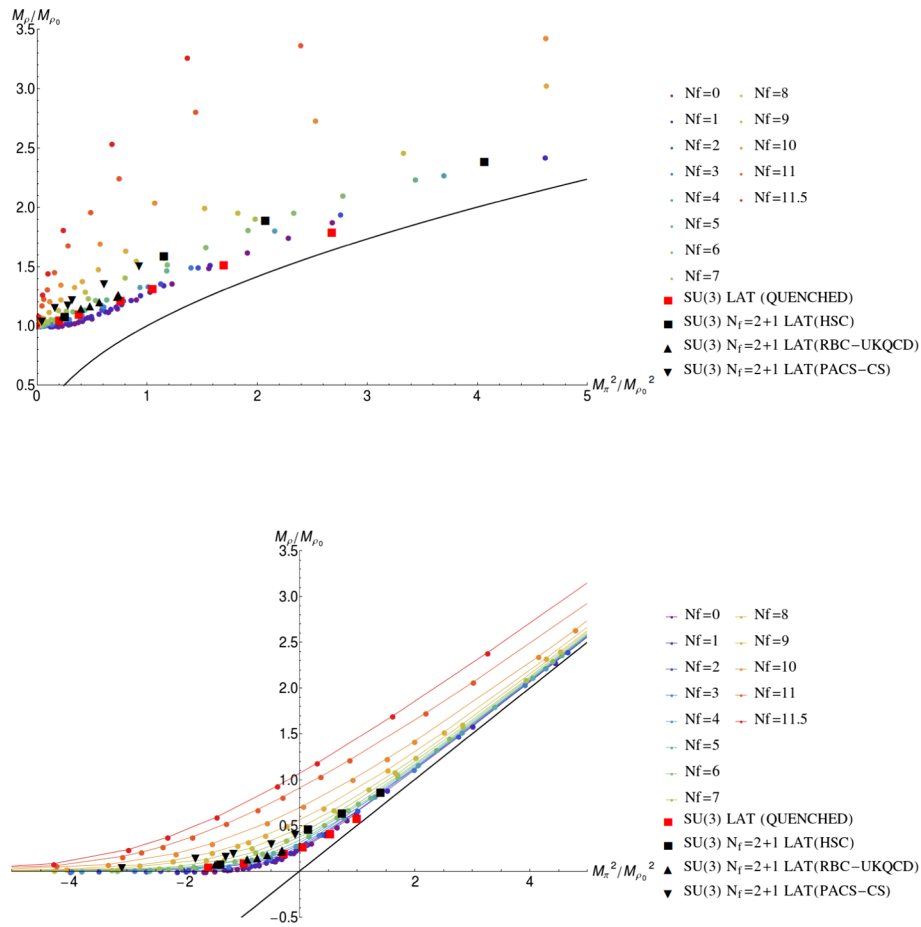


FIG. 5 (color online). SU(3) gauge theory with N_f fundamental quarks showing the approach to the conformal window at $N_f = 12$. The lower plot is a Log-Log version of the top plot. The solid line corresponds to $M_\rho = M_\pi$. The plots also show lattice data for the quenched theory [15] and unquenched $N_f = 3$ theory [21–23].

discussed in Ref. [17]. To observe this, let us now turn to computing the σ -meson mass. We will again pick $N_c = 3$ as an example and show the N_f dependence of M_σ against M_π^2 in Fig. 6. The $N_f = 7$ curve is perhaps what one would have predicted for QCD—at large quark mass, the σ and π masses become degenerate. At low quark mass, as the π mass tends to zero, the σ mass saturates at a value below the ρ mass. One might then identify this state with the $f_0(500)$ state observed in experiment. However, for $N_f = 3$, the holographic model predicts that the lightest σ is heavier than the ρ , and it looks more sensible to match it to the $f_0(980)$, which it matches at the 10% level. An explanation of the origin of the lighter f_0 would then be needed. In fact, though, the literature has considerable speculation about this state, which might be a molecule or some other exotic state (see for example Ref. [24]). We cannot resolve this issue here. However, the main use of our model is to look at significant trends in the behavior of the spectra as we adjust the running of γ . Here our plot very strongly supports the speculation that this σ mode becomes light as one approaches the walking regime and the edge of the conformal window at $N_f = 12$.

3. Other representations

As we have stressed above, dynamic AdS/QCD can accommodate a description of any arbitrary quark representation. The flavor representation enters through the

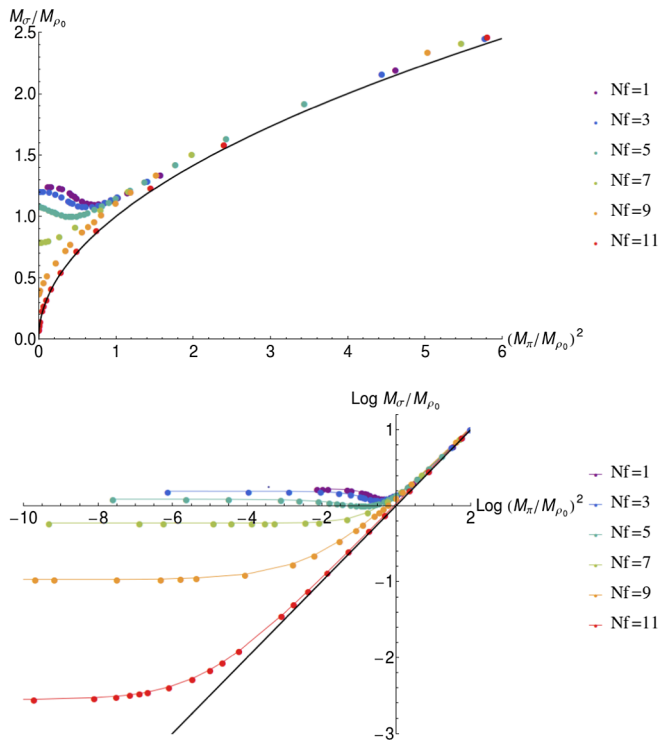


FIG. 6 (color online). M_σ versus M_π^2 in SU(3) gauge theory with varying N_f fundamental quarks. The lower plot is a Log-Log version of the top plot. The solid line corresponds to $M_\sigma = M_\pi$.

running of the anomalous dimension γ (for which we continue to use the two-loop perturbative result). In this section, we provide some plots showing some exploration of the larger space of theories.

As a first example, in Fig. 7 we show results for $N_c = 3$. The top plot shows the results in the M_ρ versus M_π^2 plane for the theory with a single quark in the fundamental representation (here the same as the 2-index antisymmetric representation), the adjoint representation, and the 2-index symmetric representation. Increasing the size of the representation makes a bigger impact on the running of the coupling and moves the curve away from QCD-like

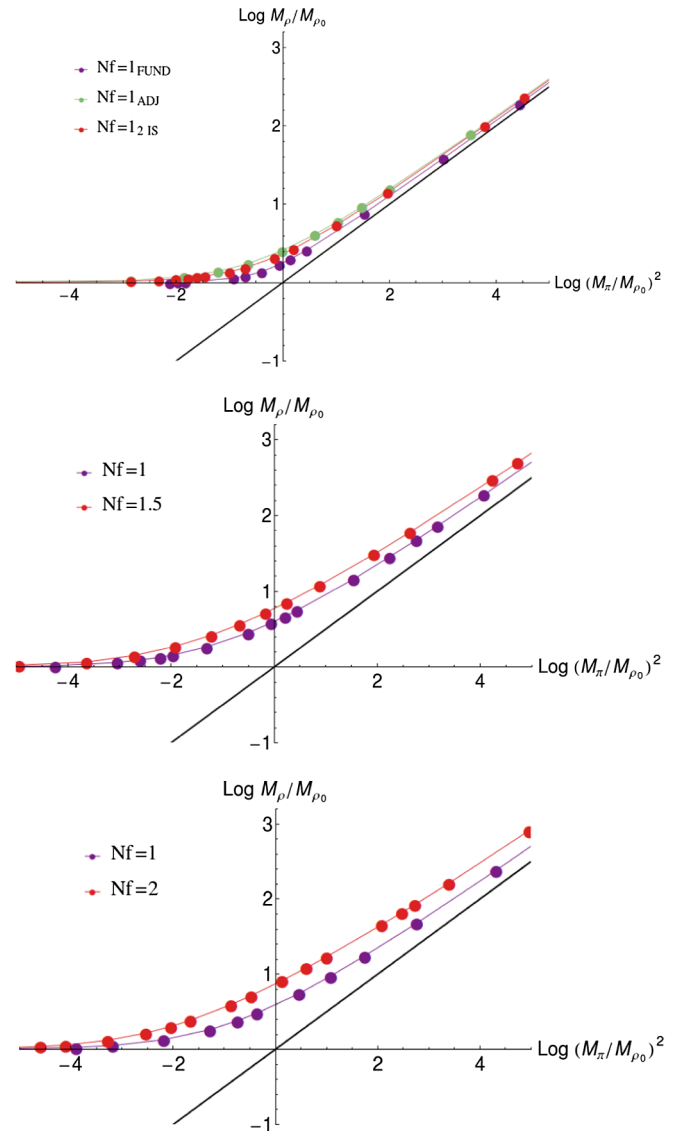


FIG. 7 (color online). A Log-Log plot in the M_ρ - M_π^2 plane for SU(3) gauge theory. The top plot shows the results in models with $N_f = 1$ but with the fermions in the fundamental, adjoint and 2-index symmetric representations. The middle figure shows the N_f dependence in the case with adjoint fermions, and the bottom plot shows the same for the 2-index symmetric representation. The solid line corresponds to $M_\sigma = M_\pi$.

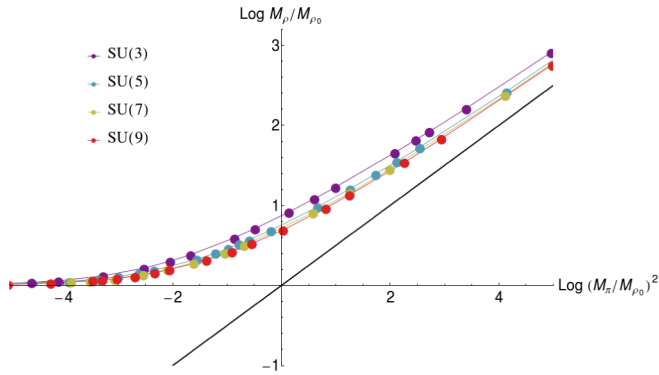


FIG. 8 (color online). A Log-Log plot in the M_ρ - M_π^2 plane for $SU(N_c)$ gauge theory with $N_f = 2$ 2-index symmetric representation quarks. The solid line corresponds to $M_\sigma = M_\pi$.

towards the walking regime. In the lower two plots, we show the N_f dependence for the adjoint and 2-index symmetric representation (here we allow $N_f = 1.5$, since by $N_f = 2$ chiral symmetry breaking is lost). Adding flavors makes the theory more walking in behavior.

We can also explore the N_c dependence of these theories at fixed N_f . For example, in Fig. 8 we vary N_c with two 2-index symmetric representation quarks. Increasing N_c moves the theory closer to the quenched limit and a more QCD-like spectrum. Within this space of theories we are not finding any additional structure beyond the dependence on the rate of running at the point $\gamma = 1$.

One final interesting case is that of 2-index antisymmetric representation quarks. As one moves to higher N_c at fixed N_f , the two-loop IR fixed point value of the coupling actually decreases. For these theories, increasing N_c moves one towards the walking regime. We show this in Fig. 9.

The walking regimes of these theories also display a light σ meson. We show this trend for a variety of sequences of theories moving towards the walking regime in Fig. 10. The trends in the spectrum as one approaches the walking regime across a wide range of theories are very similar.

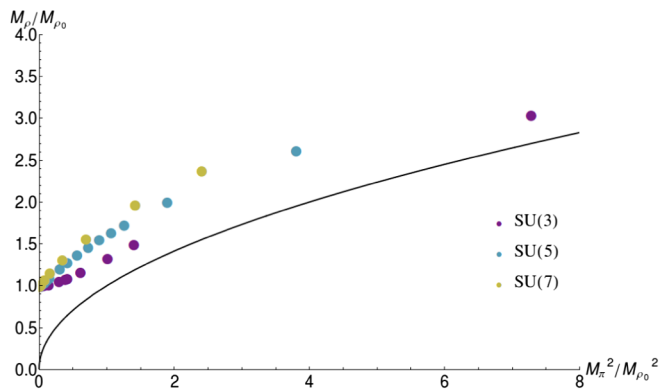


FIG. 9 (color online). A Log-Log plot in the M_ρ - M_π^2 plane for $SU(N_c)$ gauge theory with $N_f = 3$ 2-index antisymmetric representation quarks. The solid line corresponds to $M_\sigma = M_\pi$.

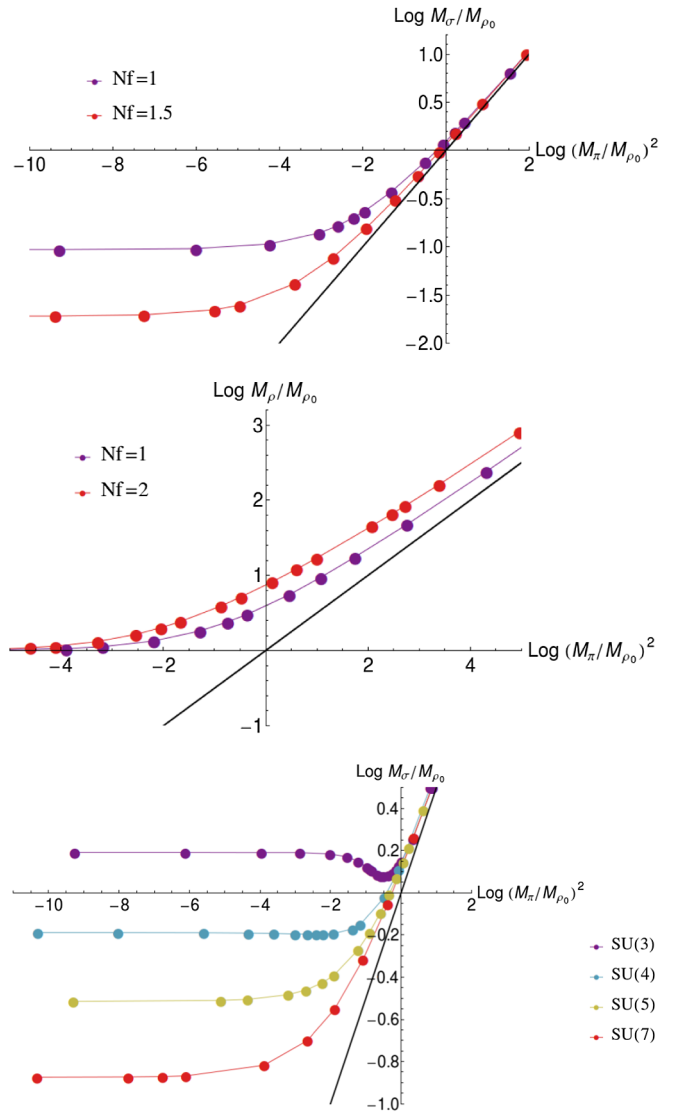


FIG. 10 (color online). Log-Log plots in the M_σ - M_π^2 plane. The top plot shows the results in $SU(3)$ gauge theory with adjoint quarks. The middle plot is for $SU(N_c)$ gauge theory with $N_f = 2$ 2-index symmetric representation quarks. The bottom plot is for $SU(N_c)$ gauge theory with $N_f = 3$ 2-index antisymmetric representation quarks. The solid line corresponds to $M_\sigma = M_\pi$.

D. The scalar glueball

Another state that one might be interested in studying as part of the lightest spectra of these theories is the lightest glueball state (see Ref. [18] for some discussions in preliminary lattice simulations). AdS/QCD is not suited to study this state, since it is fundamentally a description of the quark sector. The glueball could be included as a separate scalar in AdS, but one would then need to correctly encode its dynamics for the gauge theory's vacuum $\text{Tr} F^2$ condensate and make a guess as to how it couples in the scalar potential to the quark condensate field X . There are a lot of unknown parameters that describe the mixing of the σ and glueball state. Rather than attempt this here, we will

instead make a back-of-the-envelope computation for the glueball state.

In pure Yang-Mills, the glueball is expected to be between 5 and 10 times the one-loop strong coupling scale. In the dynamic AdS/QCD model, we have assumed the two-loop running for the gauge coupling and γ and then computed the IR quark mass gap, the value of L at the on-mass-shell condition. A simple thing to do then is to decouple the quarks at that scale $L_{\text{on-mass}}$ and use the one-loop pure Yang-Mills coupling into the IR. We compute the position of the IR pole and multiply by 8 to estimate the glueball mass. This will at least give a ballpark behavior, although mixing is explicitly not addressed.

In Fig. 11, we display the spectra of the $N_c = 3$ theory for $N_f = 3$ (QCD-like) and $N_f = 11$ (close to walking) including the glueball. Both theories display a Goldstone pion. As we have seen before, the σ becomes light and interchanges ordering with the ρ as one approaches the walking regime. In both cases, the glueball is the lightest state at large quark mass—here the quarks decouple at their mass scale, where the glue is still weakly coupled, and the pure glue theory then runs logarithmically to strong coupling at a much lower scale to set the glueball mass. For very small quark mass, the glueball becomes the heaviest state in both cases. The gauge coupling is sufficiently strong above the quark-mass scale that the BF bound is violated and the quarks acquire a dynamical mass. The pure glue running between that

scale and the IR pole is very fast, since we are already at strong coupling when the quarks decouple—the glueball mass is set by essentially the quark decoupling scale. The interesting difference between the two cases with different N_f is in the intermediate regime. The crossover between these two cases is fast for the $N_f = 3$ theory but much slower for the walking $N_f = 11$ theory. In this intermediate plateau region the walking gauge theory's coupling has run to strong coupling (although still below the value needed for chiral symmetry breaking) so the glueball mass lies close to the quark mass scale. Since it is walking, this regime, in which the quark decoupling and IR pole values are reasonably close, is enlarged in the walking theory—the crossover occurs over a wider range of quark mass. This is a signal in the spectra of walking behavior. Such a signal is important, because it does not depend on gauge-dependent objects such as the coupling itself.

IV. SUMMARY

In this paper we have studied the lowest-lying meson spectra (ρ , π , σ and the lightest glueball) in asymptotically free gauge theory using some simple holographic models. In Sec. II, we studied an old top-down model [4] that had been previously shown [3] to reproduce quenched lattice results in the M_ρ - M_π plane (see Fig. 1). The model includes strongly coupled gauge fields but returns to $\mathcal{N} = 4$ super-Yang-Mills in the UV. We argued, following Ref. [9], that the mesonic sector of the holographic model is described by a DBI action and that the only input of the background geometry is the running anomalous dimension of the quark bilinear operator, γ . We have shown that function is a good approximation to quenched QCD in Fig. 2, and this explains the success of the model in the mesonic sector.

Motivated by this observation (and the inability to find a true gravity dual of the theories under analysis), we turned to the phenomenological dynamic AdS/QCD model [8]. The model is basically the DBI action of a probe brane with the gauge dynamics input through a running scalar mass dual to γ . Once the running of γ is input, the spectrum is then predicted. Of course, we do not know the non-perturbative running of γ , but the perturbative two-loop running for the gauge coupling α combined with the one-loop expression for γ provide a well-explored proposal—these theories lose asymptotic freedom for large quark numbers and have a conformal window with a fixed point for γ at lower N_f , which rises as N_f shrinks. In the holographic setting, the condition $\gamma = 1$ corresponds to a violation of the BF bound in AdS, and the quark condensate switches on at lower values of N_f . The model then allows us to study any asymptotically free gauge theory with quarks in arbitrary representation and for any N_c and N_f —these quantities simply enter through the running of γ .

We first explored theories close to QCD—theories with a small number of quark flavors that do not impact the

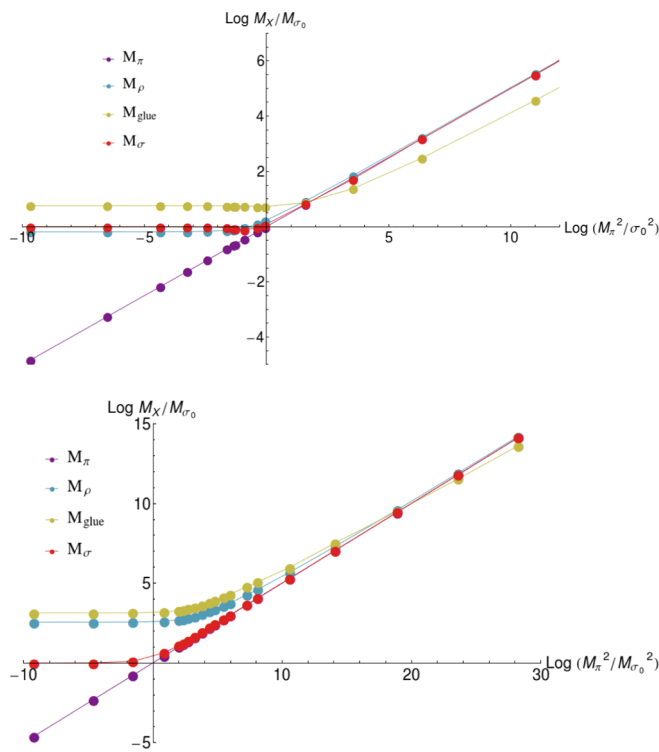


FIG. 11 (color online). The spectra of the $N_c = 3$ gauge theory with fundamental quarks: The top figure shows $N_f = 3$, the bottom $N_f = 11$.

running of the gauge coupling too much. These theories are characterized by a scale where $\gamma = 1$ and chiral symmetry breaking is triggered and a fast running of γ at that scale. They all predict a very similar mesonic spectrum (see Fig. 1, for example) that match quenched lattice predictions [15] and the top-down model previously studied, at the level of errors in the lattice computations. A variant spectrum can be seen if N_f is increased at fixed N_c , so that the theory approaches the edge of the conformal window and the running of γ is slow when $\gamma = 1$ [see, for example, the behavior in SU(3) gauge theory in Fig. 5]. The deviations are those expected given that the UV quark condensate is enhanced in these walking theories. Thus the holographic duals of walking models lead to significant deviations in the “Edinburgh” meson plots, depending on the slope of the anomalous dimension in the IR near $\gamma = 1$. However, in the QCD-like theories discussed above, these deviations are much smaller. This is due to the fact that the QCD-like models are close to the quenched limit, in which the derivative of γ has less N_f dependence at the chiral-symmetry-breaking point. The result that the deviations are much smaller in the QCD-like models as compared to the walking models adds further weight to the success of the QCD-like models in matching lattice data.

The deviation in the spectrum due to walking is the only gross feature we have found across a range of gauge theories studied. For those theories, we see the ρ mass

enhanced, the π mass enhanced to a lesser degree at a fixed bare quark mass and the σ mass falling as it acts as a Goldstone of the shift symmetry in the flattening effective potential for $\bar{q}q$. We show this behavior in Fig. 6 for SU(3) gauge theory. We explored theories with quarks in the adjoint, and two index symmetric and antisymmetric representations also, and found similar behaviors.

Finally, we estimated the lightest glueball mass in the theories, although our model does not include mixing effects with the mesonic states. At large bare quark mass, the quarks decouple at scales exponentially separated from the scale where the glue becomes strongly coupled and the glueball is light relative to the mesons. At zero quark mass, guided by QCD, the glueballs are expected to be heavier than the lightest mesons. We sketch the crossover behavior with the quark mass for SU(3) gauge theory with $N_f = 3, 11$ in Fig. 11—the effect of walking dynamics in the physical spectra is to enlarge the energy range over which this crossover occurs. This is a potentially useful statement of a signal for walking dynamics that is not couched in terms of a gauge-dependent object such as the running coupling.

ACKNOWLEDGMENTS

We thank Biagio Lucini for discussions. N. E. and M. S.’s work is supported by STFC.

-
- [1] J. M. Maldacena, The large N limit of superconformal field theories and supergravity, *Adv. Theor. Math. Phys.* **2**, 231 (1998); E. Witten, Anti-de Sitter space and holography, *Adv. Theor. Math. Phys.* **2**, 253 (1998); S. S. Gubser, I. R. Klebanov, and A. M. Polyakov, Gauge theory correlators from noncritical string theory, *Phys. Lett. B* **428**, 105 (1998).
- [2] A. Karch and E. Katz, Adding flavor to AdS/CFT, *J. High Energy Phys.* **06** (2002) 043; M. Grana and J. Polchinski, Gauge/gravity duals with holomorphic dilaton, *Phys. Rev. D* **65**, 126005 (2002); M. Bertolini, P. Di Vecchia, M. Frau, A. Lerda, and R. Marotta, $N = 2$ gauge theories on systems of fractional D3/D7 branes, *Nucl. Phys. B* **621**, 157 (2002); M. Kruczenski, D. Mateos, R. C. Myers, and D. J. Winters, Meson spectroscopy in AdS/CFT with flavor, *J. High Energy Phys.* **07** (2003) 049; V. G. Filev, C. V. Johnson, R. C. Rashkov, and K. S. Viswanathan, Flavoured large N gauge theory in an external magnetic field, *J. High Energy Phys.* **10** (2007) 019.
- [3] J. Erdmenger, N. Evans, I. Kirsch, and E. Threlfall, Mesons in gauge/gravity duals: A review, *Eur. Phys. J. A* **35**, 81 (2008).
- [4] J. Babington, J. Erdmenger, N. J. Evans, Z. Guralnik, and I. Kirsch, Chiral symmetry breaking and pions in non-supersymmetric gauge/gravity duals, *Phys. Rev. D* **69**, 066007 (2004).
- [5] J. Erlich, E. Katz, D. T. Son, and M. A. Stephanov, QCD and a holographic model of hadrons, *Phys. Rev. Lett.* **95**, 261602 (2005); L. Da Rold and A. Pomarol, Chiral symmetry breaking from five dimensional spaces, *Nucl. Phys. B* **721**, 79 (2005).
- [6] D. K. Hong and H.-U. Yee, Holographic estimate of oblique corrections for technicolor, *Phys. Rev. D* **74**, 015011 (2006); D. Arean, I. Iatrakis, M. Jarvinen, and E. Kiritsis, V-QCD: Spectra, the dilaton and the S-parameter, *Phys. Lett. B* **720**, 219 (2013); M. Jarvinen and F. Sannino, Holographic conformal window: A bottom-up approach, *J. High Energy Phys.* **05** (2010) 041; D. Arean, I. Iatrakis, and M. Jarvinen, The spectrum of (h)QCD in the Veneziano limit, *Proc. Sci., Corfu2012* (2013) 129; O. Antipin and K. Tuominen, Constraints on conformal windows from holographic duals, *Mod. Phys. Lett. A* **26**, 2227 (2011); J. Alanen and K. Kajantie, Thermodynamics of a field theory with infrared fixed point from gauge/gravity duality, *Phys. Rev. D* **81**, 046003 (2010); J. Alanen, K. Kajantie, and K. Tuominen, Thermodynamics of quasiconformal theories from gauge/gravity duality, *Phys. Rev. D* **82**, 055024 (2010); D. Kutasov, J. Lin, and A. Parnachev, Holographic walking

- from tachyon DBI, *Nucl. Phys.* **B863**, 361 (2012); M. Goykhman and A. Parnachev, S-parameter, technimesons, and phase transitions in holographic tachyon DBI models, *Phys. Rev. D* **87**, 026007 (2013).
- [7] M. Jarvinen and E. Kiritsis, Holographic models for QCD in the Veneziano Limit, *J. High Energy Phys.* **03** (2012) 002.
- [8] T. Alho, N. Evans, and K. Tuominen, Dynamic AdS/QCD and the spectrum of walking gauge theories, *Phys. Rev. D* **88**, 105016 (2013); N. Evans and M. Scott, Hyperscaling relations in the conformal window from dynamic AdS/QCD, *Phys. Rev. D* **90**, 065025 (2014).
- [9] R. Alvares, N. Evans, and K.-Y. Kim, Holography of the conformal window, *Phys. Rev. D* **86**, 026008 (2012).
- [10] P. Breitenlohner and D. Z. Freedman, Stability in gauged extended supergravity, *Ann. Phys. (N.Y.)* **144**, 249 (1982).
- [11] N. R. Constable and R. C. Myers, Exotic scalar states in the AdS/CFT correspondence, *J. High Energy Phys.* **11** (1999) 020.
- [12] W. E. Caswell, Asymptotic Behavior of Non-Abelian Gauge Theories to Two Loop Order, *Phys. Rev. Lett.* **33**, 244 (1974); T. Banks and A. Zaks, On the phase structure of vector-like gauge theories with massless fermions, *Nucl. Phys.* **B196**, 189 (1982); T. Appelquist, J. Terning, and L. C. R. Wijewardhana, The Zero-Temperature Chiral Phase Transition in SU(N) Gauge Theories, *Phys. Rev. Lett.* **77**, 1214 (1996); T. Appelquist, A. Ratnaweera, J. Terning, and L. C. R. Wijewardhana, The phase structure of an SU(N) gauge theory with N(f) flavors, *Phys. Rev. D* **58**, 105017 (1998).
- [13] T. A. Ryttov and F. Sannino, Supersymmetry inspired QCD beta function, *Phys. Rev. D* **78**, 065001 (2008); Conformal windows of SU(N) gauge theories, higher dimensional representations and the size of the unparticle world, *Phys. Rev. D* **76**, 105004 (2007); D. D. Dietrich and F. Sannino, Conformal window of SU(N) gauge theories with fermions in higher dimensional representations, *Phys. Rev. D* **75**, 085018 (2007); F. Sannino and J. Schechter, Chiral phase transition for SU(N) gauge theories via an effective Lagrangian approach, *Phys. Rev. D* **60**, 056004 (1999); A. Armoni, The conformal window from the worldline formalism, *Nucl. Phys.* **B826**, 328 (2010); H. Gies and J. Jaeckel, Chiral phase structure of QCD with many flavors, *Eur. Phys. J. C* **46**, 433 (2006).
- [14] K. C. Bowler, D. L. Chalmers, A. Kenway, R. D. Kenway, G. S. Pawley, and D. J. Wallace, A critique of quenched hadron mass calculations, *Phys. Lett.* **162B**, 354 (1985).
- [15] G. S. Bali, F. Bursa, L. Castagnini, S. Collins, L. Del Debbio, B. Lucini, and M. Panero, Mesons in large-N QCD, *J. High Energy Phys.* **06** (2013) 071.
- [16] B. Holdom, Raising the sideways scale, *Phys. Rev. D* **24**, 1441 (1981); T. Appelquist, K. D. Lane, and U. Mahanta, On the Ladder Approximation for Spontaneous Chiral Symmetry Breaking, *Phys. Rev. Lett.* **61**, 1553 (1988); A. G. Cohen and H. Georgi, Walking beyond the rainbow, *Nucl. Phys.* **B314**, 7 (1989).
- [17] K. Haba, S. Matsuzaki, and K. Yamawaki, Holographic techni-dilaton, *Phys. Rev. D* **82**, 055007 (2010); S. Matsuzaki and K. Yamawaki, Holographic techni-dilaton at 125 GeV, *Phys. Rev. D* **86**, 115004 (2012); N. Evans and K. Tuominen, Holographic modelling of a light techni-dilaton, *Phys. Rev. D* **87**, 086003 (2013); D. Elander and M. Piai, The decay constant of the holographic techni-dilaton and the 125 GeV boson, *Nucl. Phys.* **B867**, 779 (2013); D. Elander, C. Nunez, and M. Piai, A Light scalar from walking solutions in gauge-string duality, *Phys. Lett. B* **686**, 64 (2010); T. Appelquist and F. Sannino, The physical spectrum of conformal SU(N) gauge theories, *Phys. Rev. D* **59**, 067702 (1999); K. Yamawaki, M. Bando, and K. Matumoto, Scale Invariant Technicolor Model and a Technidilaton, *Phys. Rev. Lett.* **56**, 1335 (1986); M. Bando, K. Matumoto, and K. Yamawaki, Technidilaton, *Phys. Lett. B* **178**, 308 (1986); D. D. Dietrich, F. Sannino, and K. Tuominen, Light composite Higgs from higher representations versus electroweak precision measurements: Predictions for CERN LHC, *Phys. Rev. D* **72**, 055001 (2005).
- [18] L. Del Debbio and R. Zwicky, Hyperscaling relations in mass-deformed conformal gauge theories, *Phys. Rev. D* **82**, 014502 (2010); V. A. Miransky, Dynamics in the conformal window in QCD like theories, *Phys. Rev. D* **59**, 105003 (1999); T. DeGrand, Finite-size scaling tests for SU(3) lattice gauge theory with color sextet fermions, *Phys. Rev. D* **80**, 114507 (2009); B. Lucini, Strongly interacting dynamics beyond the Standard Model on a spacetime lattice, *Phil. Trans. R. Soc. A* **368**, 3657 (2010); L. Del Debbio, B. Lucini, A. Patella, C. Pica, and A. Rago, The infrared dynamics of minimal walking technicolor, *Phys. Rev. D* **82**, 014510 (2010); Mesonic spectroscopy of minimal walking technicolor, *Phys. Rev. D* **82**, 014509 (2010).
- [19] Y. Aoki, T. Aoyama, M. Kurachi, T. Maskawa, K.-i. Nagai, H. Ohki, A. Shibata, K. Yamawaki *et al.*, Many flavor QCD as exploration of the walking behavior with the approximate IR fixed point, *Proc. Sci., LATTICE2011* (2011) 080; Lattice study of conformality in twelve-flavor QCD, *Phys. Rev. D* **86**, 054506 (2012); Y. Aoki, T. Aoyama, M. Kurachi, T. Maskawa, K.-i. Nagai, H. Ohki, E. Rinaldi, A. Shibata, K. Yamawaki, and T. Yamazaki, Light Composite Scalar in Twelve-Flavor QCD on the Lattice, *Phys. Rev. Lett.* **111**, 162001 (2013); A. Cheng, A. Hasenfratz, G. Petropoulos, and D. Schaich, Scale-dependent mass anomalous dimension from Dirac eigenmodes, *J. High Energy Phys.* **07** (2013) 061; A. Deuzeman, M. P. Lombardo, T. N. da Silva, and E. Pallante, Bulk transitions of twelve flavor QCD and UA(1) symmetry, *Proc. Sci., LATTICE2011* (2011) 321; T. Appelquist, G. T. Fleming, M. F. Lin, E. T. Neil, and D. A. Schaich, Lattice simulations and infrared conformality, *Phys. Rev. D* **84**, 054501 (2011); A. Hasenfratz, Conformal or walking? Monte Carlo renormalization group studies of SU(3) gauge models with fundamental fermions, *Phys. Rev. D* **82**, 014506 (2010); Z. Fodor, K. Holland, J. Kuti, D. Negradi, and C. Schroeder, Nearly conformal gauge theories in finite volume, *Phys. Lett. B* **681**, 353 (2009); T. Appelquist, G. T. Fleming, and E. T. Neil, Lattice study of conformal behavior in SU(3) Yang-Mills theories, *Phys. Rev. D* **79**, 076010 (2009); Lattice Study of the Conformal Window in QCD-like Theories, *Phys. Rev. Lett.* **100**, 171607 (2008); **102**, 149902(E) (2009); A. Deuzeman, M. P. Lombardo, and E. Pallante, Evidence for a conformal phase in SU(N) gauge theories, *Phys. Rev. D* **82**, 074503 (2010); Y. Shamir, B. Svetitsky, and T. DeGrand, Zero of the discrete beta function

- in SU(3) lattice gauge theory with color sextet fermions, *Phys. Rev. D* **78**, 031502 (2008); Y. Iwasaki, K. Kanaya, S. Kaya, S. Sakai, and T. Yoshie, Phase structure of lattice QCD for general number of flavors, *Phys. Rev. D* **69**, 014507 (2004).
- [20] A. Karch, A. O'Bannon, and K. Skenderis, Holographic renormalization of probe D-branes in AdS/CFT, *J. High Energy Phys.* **04** (2006) 015.
- [21] H. W. Lin *et al.* (Hadron Spectrum Collaboration), First results from 2 + 1 dynamical quark flavors on an anisotropic lattice: Light-hadron spectroscopy and setting the strange-quark mass, *Phys. Rev. D* **79**, 034502 (2009).
- [22] S. Aoki *et al.* (PACS-CS Collaboration), 2 + 1 flavor lattice QCD toward the physical point, *Phys. Rev. D* **79**, 034503 (2009).
- [23] C. Allton *et al.* (RBC and UKQCD collaborations), 2 + 1 flavor domain wall QCD on a (2 fm)*83 lattice: Light meson spectroscopy with $L(s) = 16$, *Phys. Rev. D* **76**, 014504 (2007).
- [24] J.T. Londergan, J. Nebreda, J.R. Pelaez, and A. Szczepaniak, Identification of non-ordinary mesons from the dispersive connection between their poles and their Regge trajectories: The $f_0(500)$ resonance, *Phys. Lett. B* **729**, 9 (2014).